Thermal spin current and spin accumulation at ferromagnetic insulator/nonmagnetic metal interface

Y. H. Shen, X. S. Wang,* and X. R. Wang†

Physics Department, The Hong Kong University of Science and Technology, Clear Water Bay, Kowloon, Hong Kong and HKUST Shenzhen Research Institute, Shenzhen 518057, China

(Received 5 March 2016; revised manuscript received 20 May 2016; published 5 July 2016)

Spin current injection and spin accumulation near a ferromagnetic insulator (FI)/nonmagnetic metal (NM) bilayer film under a thermal gradient is investigated theoretically. By using the Fermi golden rule and the Boltzmann equations, we find that FI and NM can exchange spins via interfacial electron-magnon scattering because of the imbalance between magnon emission and absorption caused by either the deviation of the magnon number from the equilibrium Bose-Einstein distribution or the difference in magnon temperature and electron temperature. A temperature gradient in FI and/or a temperature difference across the FI/NM interface generates a spin current which carries angular momenta parallel to the magnetization of FI from the hotter side to the colder one. Interestingly, the spin current induced by a temperature gradient in NM is negligibly small due to the nonmagnetic nature of the nonequilibrium electron distributions. The results agree well with all existing experiments.

DOI: 10.1103/PhysRevB.94.014403

I. INTRODUCTION

One of the important topics in spintronics is the spin current generation and detection [1]. Compared with the electron spin current, the magnon spin current has the advantage of lower energy consumption and longer coherence time, especially in ferromagnetic insulators (FI) [2]. Furthermore, magnons can be used to manipulate the motion of magnetic domain walls [3,4]. Recently, interconversion between electron spin current and magnon spin current and various methods for magnon spin current generation in FI were proposed, such as ferromagnetic resonance (FMR) for coherent magnon spin current generation (known as spin pumping) [2,5–7] and temperature gradient for incoherent magnon spin current generation (known as spin Seebeck effect) [7–12]. The magnon spin current can be detected by a nonmagnetic metal (NM) such as Pt or Pd with strong spin-orbit coupling by which a spin current can be converted into an electric current via inverse spin Hall effect (ISHE) [13,14]. Since spin carriers in FI and NM are different (magnons in FI and electrons in NM), the spin transport and spin current conversion between electrons and magnons across the FI/NM interface becomes an interesting and important issue for both the experiment interpretation and potential applications.

Different approaches have been used to investigate the spin transport in FI/NM bilayer. The stochastic LLG equation coupled with "spin mixing conductance" concept [7,15] describes successfully how a spin current is pumped from FI into NM at FMR or under a temperature gradient [16–18]. A quantum mechanical model based on interfacial *s-d* coupling between conducting electrons in NM and local magnetic moments in FI was also proposed [19–22] for spin Seebeck effect (SSE). This model was originally designed for the transverse SSE [9,11,19]. In order to explain why spin current in NM changes direction in the higher and the lower temperature sides of a sample, coupling of phonons with spins and electrons is necessary [19] if other effect like the anomalous Nernst effect [23] was not considered. It is believed that a temperature gradient perpendicularly applied to the interface (known as *longitudinal* SSE [11,12]) is a clean configuration [23] for SSE. In this paper, we investigate the spin transport across the FI/NM interface due to interfacial electron-magnon interaction under a perpendicular temperature gradient. Phonons do not dominate spin transport in this case and are neglected. We show that there is neither spin accumulation nor spin current at thermal equilibrium, consistent with the laws of thermodynamics. Once there is a temperature gradient in the sample or a temperature difference at the interface, spin accumulation occurs and a spin current flows across the interface. Spins parallel to the magnetization of FI flow from the hotter side to the colder one under a temperature gradient in FI or under a temperature difference across the interface. Surprisingly, a temperature gradient in NM cannot efficiently generate a spin current because the spin currents from nonequilibrium spin-up electrons and spin-down electrons cancel each other, resulting in a negligible contribution. Our results are in good agreement with the present experiments.

II. MODEL AND INTERFACIAL ELECTRON-MAGNON SCATTERING

Following the longitudinal SSE experiments [11], we consider a FI/NM bilayer model as shown in Fig. 1(a). An NM layer is in contact with a FI layer, and two thermal reservoirs of temperatures T_L and T_R are attached to the left side of NM and the right side of FI. The volume, thickness, and lattice constant of FI and NM layers are denoted by V_i, d_i, and b_i (i = FI, NM). The interface is in the yz plane and its area is A. Although most insulators used in SSE experiments are ferrimagnetic, the energies of intersublattice excitations (optical magnons) are too high to be excited at low temperature [19,24]. Only the acoustic spin waves are relevant so that FIs are considered. A FI can be modeled by the Heisenberg model of spin S on the cubic

*Corresponding author: justicewxs@ust.hk
†Corresponding author: phxwan@ust.hk

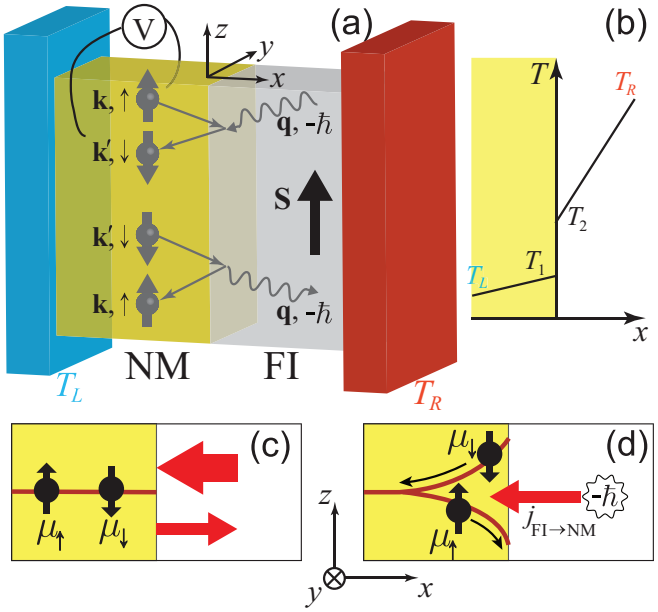

FIG. 1. (a) The setup of a FI/NM bilayer model and possible electron-magnon scattering process at the interface: A spin-up (spin-down) electron of wave vector $\mathbf{k}$ ($\mathbf{k}'$) becomes a spin-down (spin-up) electron of wave vector $\mathbf{k}'$ ($\mathbf{k}$) after absorbing (emitting) a magnon of wave vector $\mathbf{q}$. NM (left) and FI layers (right) are colored yellow and white. The blue and red blocks denote, respectively, thermal reservoirs of temperature T_L and T_R. (b) Schematic diagram of the temperature profile when $T_R > T_L$. (c) The instant when FI and NM are brought in contact. More magnons flow to the left (thicker arrow) than those to the right (thinner arrow). (d) At the steady state under a thermal gradient, spins flow across the interface and spin accumulation occurs in NM near the FI/NM interface. Spin angular momentum along the $-z$ direction flows from the hotter side to the colder side.

lattice. The electrons in NM are modeled as a free-electron gas. Without losing generality, magnetization of FI is in the $-z$ direction so that atomic spins $\mathbf{S}$ are in the $+z$ direction due to the negative gyromagnetic ratio. The z component of spins carried by spin-up (spin-down) electrons and magnons are $\frac{\hbar}{2}$ ($-\frac{\hbar}{2}$) and $-\hbar$, respectively, in our model. The current density of spins along the z direction in NM is $\mathbf{j}_s = (\frac{\hbar}{2e})\mathbf{j}_\uparrow - (\frac{\hbar}{2e})\mathbf{j}_\downarrow$, where $\mathbf{j}_{\uparrow(\downarrow)}$ is the electric current density carried by spin-up (spin-down) electrons and $e > 0$ is the absolute value of the electron charge.

The interaction between electrons in NM and local magnetic moment is modeled by an interfacial s-d Hamiltonian [25,26],

$$H = -\mathcal{J}_{sd} b_{\rm FI}^3 \sum_n \mathbf{s}(\mathbf{r}) \cdot \mathbf{S}_n \delta(\mathbf{r} - \mathbf{R}_n), \tag{1}$$

where $\mathbf{s}(\mathbf{r})$ is itinerant electron spin in NM at position $\mathbf{r}$ and $\mathbf{S}_n$ is local atomic spin at site n of position $\mathbf{R}_n$ on the interface. $\mathbf{s}$ and $\mathbf{S}_n$ are in the units of $\hbar$. $\mathcal{J}_{sd}$ is the s-d coupling strength and the summation is over the atom sites on the interface. To calculate the interfacial electron-magnon scattering rate, we use the lowest-order Holstein-Primakoff transformation [27] $S_{n-} = \sqrt{2S}a_n^\dagger$ and $S_{n+} = \sqrt{2S}a_n$ (S_{n+} and S_{n-} are ladder operators of $\mathbf{S}_n$ at site n and $a_n^\dagger$,a_n are the corresponding creation and annihilation operators of magnons) so that magnon-magnon interactions are neglected. The scattering due to the non-spin-flipping part of H does not contribute to spin current and spin accumulation and is neglected. In the momentum space, H involving spin flipping can be written as,

$$H' = -\mathcal{J}_{sd} \frac{b_{\rm FI}^3 N_{\rm IN}}{V_{\rm NM}} \sqrt{\frac{S}{2N_{\rm FI}}} \times \sum_{\mathbf{k},\mathbf{k}',\mathbf{q}} (c_{\mathbf{k}'\uparrow}^\dagger c_{\mathbf{k}\downarrow} a_{\mathbf{q}}^\dagger + c_{\mathbf{k}'\downarrow}^\dagger c_{\mathbf{k}\uparrow} a_{\mathbf{q}}) \delta_{\mathbf{k}'_\parallel - \mathbf{k}_\parallel = \mathbf{q}_\parallel}, \tag{2}$$

where $c_{\mathbf{k}\uparrow}^\dagger$ ($c_{\mathbf{k}\uparrow}$) and $c_{\mathbf{k}\downarrow}^\dagger$ ($c_{\mathbf{k}\downarrow}$) are the creation (annihilation) operators of spin-up and spin-down electrons of wave vector $\mathbf{k}$, respectively. $a_{\mathbf{q}}^\dagger$ ($a_{\mathbf{q}}$) is the creation (annihilation) operator of magnons of wave vector $\mathbf{q}$. $N_{\rm FI}$ and $N_{\rm IN}$ are the numbers of atomic spins in FI and at the interface, respectively. The first (second) term describes an incident spin-down (spin-up) electron of wave vector $\mathbf{k}'$ ($\mathbf{k}$) emitting (absorbing) a magnon of wave vector $\mathbf{q}$ and becoming an outgoing spin-up (spin-down) electron of wave vector $\mathbf{k}$ ($\mathbf{k}'$), as illustrated in Fig. 1(a). This Hamiltonian preserves angular momentum, and the momentum parallel to the interface is conserved.

Similar to the usual phonon-electron scattering calculation [28] by the Fermi golden rule, the magnon emission and absorption rates between electron states $\mathbf{k}$ and $\mathbf{k}'$ are

$$t_{\rm em} = \frac{\pi S \mathcal{J}_{sd}^2 b_{\rm FI}^6 N_{\rm IN}^2}{\hbar V_{\rm NM}^2 N_{\rm FI}} [n(\mathbf{q}) + 1] \delta(E_{\mathbf{k}} + \varepsilon_{\mathbf{q}} - E_{\mathbf{k}'}) \delta_{\mathbf{k}'_\parallel - \mathbf{k}_\parallel = \mathbf{q}_\parallel},$$

$$t_{\rm ab} = \frac{\pi S \mathcal{J}_{sd}^2 b_{\rm FI}^6 N_{\rm IN}^2}{\hbar V_{\rm NM}^2 N_{\rm FI}} n(\mathbf{q}) \delta(E_{\mathbf{k}} + \varepsilon_{\mathbf{q}} - E_{\mathbf{k}'}) \delta_{\mathbf{k}'_\parallel - \mathbf{k}_\parallel = \mathbf{q}_\parallel},$$

where $n(\mathbf{q})$ is the number of magnons of wave vector $\mathbf{q}$, $E_{\mathbf{k}}$ and $\varepsilon_{\mathbf{q}}$ are electron energy of wave vector $\mathbf{k}$ and magnon energy of wave vector $\mathbf{q}$, respectively. According to the physical picture illustrated in Fig. 1(a), the perpendicular wavevector components should satisfy $k'_x > 0, k_x < 0, q_x > 0$ for magnon emission and $k_x > 0, k'_x < 0$, $q_x < 0$ for absorption. For simplicity, a quadratic dispersion is assumed for electrons in NM, $E_{\mathbf{k}} = \frac{\hbar^2 |\mathbf{k}|^2}{2m}$. The magnon spectrum is $\varepsilon_{\mathbf{q}} = J|\mathbf{q}|^2 + D$ where J is the ferromagnetic exchange coupling and D is the gap due to magnetic anisotropy.

The net spin current density $j_{\rm FI\to NM}$ at the interface is defined as the angular momentum parallel to the magnetization of FI across the interface per unit area and per unit time, which is proportional to the difference of the absorbed magnon number $N_{\rm ab}$ and the emitted one $N_{\rm em}$ per unit time,

$$j_{\rm FI\to NM} = \hbar \frac{N_{\rm ab} - N_{\rm em}}{A}. \tag{3}$$

By including the Pauli principle for electrons, $N_{\rm ab}$ and $N_{\rm em}$ can be obtained from $t_{\rm ab}$ and $t_{\rm em}$,

$$N_{\rm em} = \sum_{\mathbf{k},\mathbf{k}',\mathbf{q}} f_\downarrow(\mathbf{k}')[1 - f_\uparrow(\mathbf{k})] t_{\rm em},$$
$$N_{\rm ab} = \sum_{\mathbf{k},\mathbf{k}',\mathbf{q}} f_\uparrow(\mathbf{k})[1 - f_\downarrow(\mathbf{k}')] t_{\rm ab}, \tag{4}$$

where $f_s(\mathbf{k})$ is the electron distribution function of wave vector $\mathbf{k}$ and spin $s = \uparrow,\downarrow$. For a macroscopic system the summation can be converted into integration by $\sum_{\mathbf{k},\mathbf{k}',\mathbf{q}} \delta_{\mathbf{k}'_\parallel - \mathbf{k}_\parallel = \mathbf{q}_\parallel} \rightarrow \frac{V_{\rm NM}}{(2\pi)^3}\frac{V_{\rm NM}}{(2\pi)^3}\frac{d_{\rm FI}}{2\pi}\int \delta(\mathbf{k}_\parallel + \mathbf{q}_\parallel - \mathbf{k}'_\parallel)\mathrm{d}\mathbf{k}\mathrm{d}\mathbf{k}'\mathrm{d}\mathbf{q}$. The range of integration is $k_x > 0, k'_x < 0, q_x < 0$ for magnon absorption and $k'_x > 0, k_x < 0, q_x > 0$ for emission. $\mathbf{q}$ is in the first Brillioun zone. To combine two integrals in Eq. (4) together, we change the dummy variables in $N_{\rm em}$ as $\mathbf{k} \rightarrow -\mathbf{k}$, $\mathbf{k}' \rightarrow -\mathbf{k}'$, and $\mathbf{q} \rightarrow -\mathbf{q}$. The spin current becomes

$$j_{\rm FI\rightarrow NM} = \hbar C \int_{\rm all} \{f_\uparrow(\mathbf{k})[1 - f_\downarrow(\mathbf{k}')]n(\mathbf{q}) - f_\downarrow(-\mathbf{k}')[1 - f_\uparrow(-\mathbf{k})][n(-\mathbf{q}) + 1]\} \quad (5)$$

with $C = \frac{\pi}{\hbar}\frac{S\mathcal{J}_{sd}^2 b_{\rm FI}^5}{(2\pi)^7}$. Here $\int_{\rm all} = \int \delta(E_\mathbf{k} + \varepsilon_\mathbf{q} - E_{\mathbf{k}'})\delta(\mathbf{k}_\parallel + \mathbf{q}_\parallel - \mathbf{k}'_\parallel)\mathrm{d}\mathbf{k}\mathrm{d}\mathbf{k}'\mathrm{d}\mathbf{q}$ with $k_x > 0$, $k'_x < 0, q_x < 0$, and $\mathbf{q} \in$ Brillioun zone.

III. SPIN TRANSPORT AT THERMAL EQUILIBRIUM

First we consider the case of the bilayer at thermal equilibrium ($T_L = T_R = T$). The magnon number follows the Bose-Einstein distribution $n(\mathbf{q}) = n_0(\mathbf{q}) = \frac{1}{e^{\beta\varepsilon_\mathbf{q}} - 1}$ and the electron distribution function is the Fermi-Dirac function $f_s(\mathbf{k}) = f_0(\mathbf{k}) = \frac{1}{e^{\beta(E_\mathbf{k} - \mu_s)} + 1}$, where $s = \uparrow,\downarrow, \beta = (k_B T)^{-1}$ and k_B is the Boltzmann constant. Because electrons are unpolarized in NM, the chemical potentials of spin-up and spin-down electrons must be the same, $\mu_\uparrow = \mu_\downarrow = \mu_0$, at the instant when FI and NM are brought to contact. Due to the energy conservation $E_\mathbf{k} + \varepsilon_\mathbf{q} = E_{\mathbf{k}'}$, we have

$$\begin{aligned} & f_0(\mathbf{k})[1 - f_0(\mathbf{k}')]n_0(\mathbf{q}) \\ &= \frac{1}{e^{\beta(E_\mathbf{k} - \mu_0)} + 1}\frac{e^{\beta(E_{\mathbf{k}'} - \mu_0)}}{e^{\beta(E_{\mathbf{k}'} - \mu_0)} + 1}\frac{1}{e^{\beta\varepsilon_\mathbf{q}} - 1} \\ &= \frac{1}{e^{\beta(E_\mathbf{k} - \mu_0)} + 1}\frac{e^{\beta(E_\mathbf{k} - \mu_0)}e^{\beta\varepsilon_\mathbf{q}}}{e^{\beta(E_{\mathbf{k}'} - \mu_0)} + 1}\frac{1}{e^{\beta\varepsilon_\mathbf{q}} - 1} \\ &= f_0(-\mathbf{k}')[1 - f_0(-\mathbf{k})][n_0(-\mathbf{q}) + 1]. \end{aligned} \quad (6)$$

Equation (6) is the detailed balance between magnon absorption and magnon emission at the thermal equilibrium. Using this detailed balance result, Eq. (5) gives a vanishing spin current, $j_{\rm FI\rightarrow NM} = 0$, and no spin accumulation in this case. In fact, no spin current and no spin accumulation at the thermal equilibrium hold in general. Otherwise, a spin current would convert into charge current via the ISHE. Thus, this device would generate electricity at the thermal equilibrium. Since no external energy source exists in the set-up, this assumption leads to a continuous extraction of electric energy from a sole heat bath, a clear violation of the second law of thermodynamics. Thus, our result must be model independent and true in general. However, this result does not contradict those proposals of persistent spin Hall current in dissipationless systems [29]. The second law of thermodynamics is not violated there because the energy is not dissipated by the persistent current in those systems. Also, the magnon-electron scattering cannot induce magnetism in NM at the thermal equilibrium because of the absence of spin accumulation. This is different from the equilibrium "proximity effect" in some systems, such as a semiconductor carbon nanotube in contact with a metallic carbon nanotube [30]. There, the semiconductor carbon nanotube becomes a weak metal at the thermal equilibrium.

IV. SPIN TRANSPORT AT NONEQUILIBRIUM

When different temperatures T_L, T_R are applied on the two sides of the FI/NM bilayer as shown in Fig. 1(a), the system is at a nonequilibrium state and thermal gradients will eventually be established in both FI and NM. Also, a temperature difference across the FI/NM interface may exist when the thermal contact resistance is nonzero. The temperature profile can in principle be obtained by solving the corresponding heat diffusion equations with proper boundary conditions if the thermal conductivities and other material parameters are known. Since the temperature profile is not the subject of this paper, we shall simply assume constant thermal conductivities κ_i of the materials (i = FI,NM) and a constant thermal contact resistance R [11,31,32]. Thus, as shown in Fig. 1(b), a uniform temperature gradient of $\alpha_{\rm NM} = (T_1 - T_L)/d_{\rm NM}$ in NM, a uniform temperature gradient of $\alpha_{\rm FI} = (T_R - T_2)/d_{\rm FI}$ in FI, and an interfacial temperature difference $\Delta T \equiv T_2 - T_1$ across the interface are established at the steady state. $\alpha_{\rm NM}$, $\alpha_{\rm FI}$, and ΔT satisfy

$$\alpha_{\rm NM} d_{\rm NM} + \Delta T + \alpha_{\rm FI} d_{\rm FI} = T_R - T_L,$$
$$\alpha_{\rm NM}\kappa_{\rm NM} = \frac{\Delta T}{R} = \alpha_{\rm FI}\kappa_{\rm FI}.$$

$\alpha_{\rm NM}$ will induce a nonequilibrium distribution of electrons, while $\alpha_{\rm FI}$ will induce a nonequilibrium distribution of magnons. ΔT will break the detailed balance between the magnon absorption and emission as shown in Sec. III. Since the magnon emission and absorption are no longer balanced, a net spin current across the interface shall appear.

On the other hand, due to the spin conserved s-d interaction at the interface, each absorbed magnon results in an electron to flip from spin-up to spin-down state, and each emitted magnon causes an electron to flip from spin-down to spin-up state. Thus, if there are more absorbed magnons than emitted ones [$j_{\rm FI\rightarrow NM} > 0$ according to Eq. (3)], the number of spin-down electrons would be larger than that of spin-up electrons, and chemical potential of spin-up and spin-down electrons would no longer be the same and $\mu_\downarrow > \mu_\uparrow$. Similarly, when $j_{\rm FI\rightarrow NM} < 0$, we have $\mu_\uparrow > \mu_\downarrow$. The electron spin accumulation near the interface causes a spin current $\mathbf{j}_s$ in NM due to spin diffusion. This spin current should be continuum at the interface. Thus we have

$$-j_{\rm FI\rightarrow NM} = j_s(0) = \left(\frac{\hbar}{2e}\right)j_\uparrow(0) + \left(-\frac{\hbar}{2e}\right)j_\downarrow(0). \quad (7)$$

Both $j_{\uparrow(\downarrow)}$ and $j_{\rm FI\rightarrow NM}$ can be determined by the distribution functions of electrons and magnons, which will be studied by solving the Boltzmann equations in the next subsection.

A. Distribution functions under a given temperature profile

When the system is not far from the equilibrium, $n(\mathbf{q})$ and $f_s(\mathbf{k})$ ($s = \uparrow,\downarrow$) are governed by the Boltzmann equations with the relaxation time approximation. For magnons, the distribution function $n(\mathbf{q})$ under the thermal gradient $\alpha_{\rm FI}$ can

be obtained by solving the following Boltzmann equation

$$\mathbf{v}(\mathbf{q})\cdot\nabla n(\mathbf{q}) = -\frac{n_1(\mathbf{q})}{\tau}, \tag{8}$$

where $\mathbf{v}(\mathbf{q}) = \frac{1}{\hbar}\nabla_{\mathbf{q}}\varepsilon_q$ is the group velocity of magnons with wavevector $\mathbf{q}$, τ is the average relaxation time of magnons, and $n_1(\mathbf{q}) = n(\mathbf{q}) - n_0(\mathbf{q})$ where $n_0(\mathbf{q}) = \frac{1}{e^{\beta\varepsilon_q}-1}$ is the Bose-Einstein distribution with the local temperature. To the first order in $\alpha_{\rm FI}$, we can replace $n(\mathbf{q})$ by $n_0(\mathbf{q})$ in Eq. (8) and obtain

$$n(\mathbf{q}) = n_0(\mathbf{q}) - \tau v_x(\mathbf{q})\alpha_{\rm FI}\frac{\partial n_0(\mathbf{q})}{\partial T}, \tag{9}$$

where $\frac{\partial n_0}{\partial T} = \frac{\beta\varepsilon_q}{T}n_0(n_0+1)$. Obviously, we have $n_1(-\mathbf{q}) = -n_1(\mathbf{q})$.

In the discussion above, magnon lifetime is assumed to be very short so that its chemical potential is zero like phonons and photons. In reality, the lifetime of quasiparticles is finite. The magnon chemical potential is nonzero under external pumping [20,33] when the magnon lifetime is longer than the thermalization time. This is why Bose-Einstein condensation was indeed observed for magnons [33] as well as for excitons. Although the quantitative results would be modified when magnon lifetime is long, the physics reported here do not change. Quantitatively, the spin current generated by ΔT is slightly larger for nonzero magnon chemical potential than that with zero one. The spin current generated by the temperature gradient in FI is almost not affected at the low temperatures (<40 K) but much lower for nonzero magnon chemical potential at higher temperatures. The nonzero magnon chemical potential has two opposite effects as we will see in the Appendix.

For electrons, the nonequilibrium distribution is not only affected by the temperature gradient $\alpha_{\rm NM}$ but also by the spin accumulation near the interface, as shown in Fig. 1(d). To take this spin accumulation into consideration, we need to solve the Boltzmann equation about $f_s(\mathbf{k},\mathbf{r})$ including the spin-flip process [21,34,35]:

$$\mathbf{v}\cdot\nabla f_s + \left(-\frac{e\boldsymbol{\mathcal{E}}}{\hbar}\right)\cdot\nabla_{\mathbf{k}} f_s = -\frac{f_s - f_{0,s}}{\tau_c} - \frac{f_{0,s} - f_{0,-s}}{\tau_{sf}}, \tag{10}$$

where $\mathbf{v} = \frac{\hbar\mathbf{k}}{m}$, $f_{0,s} = [e^{\beta(E-\mu_s)}+1]^{-1}$ is the equilibrium distribution function with local temperature and local electrochemical potential $\mu_s(x)$ for spin s. The relaxation times τ_c and τ_{sf} describe, respectively, the momentum-energy relaxation and spin relaxation of electrons. $\boldsymbol{\mathcal{E}} = -\nabla\phi$ is the electric field in NM, and $E = \frac{\hbar^2k^2}{2m} - e\phi$ is the electron energy. To solve Eq. (10) in the linear response regime ($f_{1,s}$ linear in the temperature gradient and electric field), we can replace f_s by $f_{0,s}$ in the left-hand side of Eq. (10). Thus, we obtain

$$\mathbf{v}\cdot\left[\frac{-\nabla T}{T}(E-\mu_s) - \nabla\mu_s\right]\frac{\partial f_{0,s}}{\partial E} = -\frac{f_s - f_{0,s}}{\tau_c} - \frac{f_{0,s} - f_{0,-s}}{\tau_{sf}}. \tag{11}$$

Normally, the deviation of the local electrochemical potential $\delta\mu_s = \mu_s - \mu_e$ from the electrochemical potential without spin accumulation (μ_e) is small. Since the change of the density of state near the Fermi surface is small, it is common to use the approximation of $\delta\mu_\uparrow = -\delta\mu_\downarrow$ [21,36,37]. After expanding μ_s and $f_{0,s}$ at μ_e and keeping the linear terms in Eq. (11), we have

$$f_s(\mathbf{k}) = f_0(\mathbf{k}) - \left(1 - 2\frac{\tau_c}{\tau_{sf}}\right)\delta\mu_s\frac{\partial f_0(\mathbf{k})}{\partial E} + g_s(\mathbf{k}), \tag{12}$$

where

$$g_s(\mathbf{k}) = \tau_c v_x(\mathbf{k})\left[\frac{\alpha_{\rm NM}}{T}(E_k - \mu_e) + \frac{{\rm d}\mu_e}{{\rm d}x} + \frac{{\rm d}\delta\mu_s}{{\rm d}x}\right]\frac{\partial f_0(\mathbf{k})}{\partial E},$$

and $f_0 = [e^{\beta(E-\mu_e)}+1]^{-1}$ is the Fermi-Dirac distribution function without spin accumulation. Because $\tau_c \ll \tau_{sf}$ in most cases, we can discard $2\frac{\tau_c}{\tau_{sf}}$ in Eq. (12). Obviously, we have $g_s(-\mathbf{k}) = -g_s(\mathbf{k})$ and $f_{1,s}(\mathbf{k}) = f_s(\mathbf{k}) - f_0(\mathbf{k}) = -\delta\mu_s\frac{\partial f_0(\mathbf{k})}{\partial E} + g_s(\mathbf{k})$.

Since $\frac{{\rm d}\mu_e}{{\rm d}x}$ and $\frac{{\rm d}\delta\mu_\uparrow}{{\rm d}x} = -\frac{{\rm d}\delta\mu_\downarrow}{{\rm d}x}$ are still unknown, we need to consider the charge/spin transport in NM. In NM where $(f_\uparrow + f_\downarrow) = 2f_0 + 2\tau_c v_x[\frac{\alpha_{\rm NM}}{T}(E-\mu_e) + \frac{{\rm d}\mu_e}{{\rm d}x}]\frac{\partial f_0}{\partial E}$, the electric current

$$j = \frac{(-e)}{V_{\rm NM}}\sum_{\mathbf{k}} 2\tau_c v_x^2\left[\frac{\alpha_{\rm NM}}{T}(E-\mu_e) + \frac{{\rm d}\mu_e}{{\rm d}x}\right]\frac{\partial f_0}{\partial E} \tag{13}$$

is not affected by the spin accumulation, and the spin current

$$j_s = -\frac{\hbar}{2V_{\rm NM}}\sum_{\mathbf{k}} v_x(f_\uparrow - f_\downarrow) = \frac{\hbar\sigma}{2e^2}\frac{{\rm d}\delta\mu_\uparrow}{{\rm d}x} \tag{14}$$

depends on the spin accumulation. $\sigma = \frac{ne^2\tau_c}{m}$ is the conductivity of the metal, n is the electron density in the NM.

The distribution of $\delta\mu_\uparrow$ inside NM can be determined by the diffusion equation [21,34–37]:

$$\frac{{\rm d}^2\delta\mu_\uparrow}{{\rm d}x^2} = \frac{\delta\mu_\uparrow}{l_{sd}^2},$$

where l_{sd} is the spin diffusion length. For $d_{\rm NM} \gg l_{sd}$, $\delta\mu_\uparrow(x) = \delta\mu_\uparrow(0)\exp(x/l_{sd})$, and

$$\frac{{\rm d}\delta\mu_\uparrow}{{\rm d}x} = \frac{\delta\mu_\uparrow}{l_{sd}}. \tag{15}$$

$\frac{{\rm d}\mu_e}{{\rm d}x}$ can be determined from the fact that there is no electric current in an open circuit; Eq. (13) gives

$$\frac{{\rm d}\mu_e}{{\rm d}x} = -\frac{\alpha_{\rm NM}\int v^2(E-\mu_e)\frac{\partial f_0}{\partial E}{\rm d}^3\mathbf{k}}{T\int v^2\frac{\partial f_0}{\partial E}{\rm d}^3\mathbf{k}} \approx -\frac{\alpha_{\rm NM}}{2T}\frac{(\pi k_{\rm B}T)^2}{\mu_e}. \tag{16}$$

This is the conventional Seebeck effect [38].

To fully determine $f_s(\mathbf{k})$, one still needs to find out $\delta\mu_\uparrow(0)$ in terms of known model parameters. The right hand side of Eq. (7) is linear in $\delta\mu_\uparrow(0)$ after using the expression found early for j_s and $\frac{{\rm d}\delta\mu_\uparrow}{{\rm d}x} = \frac{\delta\mu_\uparrow}{l_{sd}}$. $j_{\rm FI\to NM}$ in Eq. (7) can also be expressed by $n(\mathbf{q})$ and $f_s(\mathbf{k})$ as given by Eq. (5). Thus Eq. (7) would be an equation about $\delta\mu_\uparrow(0)$. Then we can obtain the spin

accumulation and spin current across the interface as shown below.

B. Spin current in linear response regime

In the last subsection, we obtained $f_s(\mathbf{k}) = f_0(\mathbf{k}) + f_{1,s}(\mathbf{k})$ and $n(\mathbf{q}) = n_0(\mathbf{q}) + n_1(\mathbf{q})$, where $f_{1,s}$ and n_1, linear in thermal gradient, is much smaller than their equilibrium values. Substitute them into Eq. (5) and keep only the terms up to linear orders in $f_{1,s}$ and n_1, the spin current can be decomposed into three terms:

$$j_{\mathrm{FI}\to\mathrm{NM}} = j_d + j_m + j_e, \tag{17}$$

where

$$\begin{aligned} j_d &= \hbar C \int_{\mathrm{all}} \{f_0(\mathbf{k})[1 - f_0(\mathbf{k}')]n_0(\mathbf{q}) \\ &\quad - f_0(\mathbf{k}')[1 - f_0(\mathbf{k})][n_0(\mathbf{q}) + 1]\}, \end{aligned} \tag{18}$$

$$\begin{aligned} j_m &= \hbar C \int_{\mathrm{all}} \{f_0(\mathbf{k})[1 - f_0(\mathbf{k}')]n_1(\mathbf{q}) \\ &\quad - f_0(\mathbf{k}')[1 - f_0(\mathbf{k})]n_1(-\mathbf{q})\}, \end{aligned} \tag{19}$$

$$\begin{aligned} j_e &= \hbar C \int_{\mathrm{all}} \{f_{1,\uparrow}(\mathbf{k})[1 - f_0(\mathbf{k}')] - f_0(\mathbf{k}) f_{1,\downarrow}(\mathbf{k}')\} n_0(\mathbf{q}) \\ &\quad - \{f_{1,\downarrow}(-\mathbf{k}')[1 - f_0(\mathbf{k})] - f_0(\mathbf{k}') f_{1,\uparrow}(-\mathbf{k})\}[n_0(\mathbf{q}) + 1], \end{aligned} \tag{20}$$

where $f_0 = \frac{1}{e^{\beta_1(E-\mu_e)}+1}$ and $n_0 = \frac{1}{e^{\beta_2\varepsilon}-1}$ with $\beta_1 = \frac{1}{k_B T_1}$, $\beta_2 = \frac{1}{k_B T_2}$. T_1 and T_2 are the temperatures of NM and FI at the FI/NM interface.

Since Eq. (6) is no longer valid if $\beta_1 \neq \beta_2$, j_d is not zero in this case. j_m is mainly due to the deviation of magnons from their equilibrium distribution. If there is no temperature gradient α_{FI}, Eq. (9) says $n_1 = 0$, and then j_m vanishes. j_e comes from the deviation of electrons from their equilibrium distribution. According to Eq. (12), the deviation is caused by both temperature gradient α_{NM} as well as the spin accumulation $\delta\mu\uparrow$ originated from the spin injection across the interface. Even if $\alpha_{\mathrm{NM}} = 0$, $f_{1,s}$ still exists as long as there is a nonzero spin current, for example from $\Delta T = T_2 - T_1 \neq 0$ or $\alpha_{\mathrm{FI}} \neq 0$. Below, we will study j_d, j_m, j_e separately, and by applying the boundary condition given in Eq. (7), and find out the relationship between spin current across the interface, spin accumulation at steady state and $\Delta T, \alpha_{\mathrm{FI}}, \alpha_{\mathrm{NM}}$. To simplify the presentation, we introduce two notations

$$\begin{aligned} L_1 &= f_0(\mathbf{k})[1 - f_0(\mathbf{k}')]n_0(\mathbf{q}), \\ L_2 &= f_0(\mathbf{k}')[1 - f_0(\mathbf{k})][n_0(\mathbf{q}) + 1]. \end{aligned} \tag{21}$$

Then, $j_d = \hbar C \int_{\mathrm{all}}(L_1 - L_2)$, where $L_1/L_2 = e^{(\beta_1-\beta_2)\varepsilon_q}$. When $T_2 > T_1$, the magnons have higher temperature, we have $\beta_1 > \beta_2, L_1 > L_2$, and $j_d > 0$. The spin current induced by the temperature difference flows from FI to NM. The spin current reverses its direction when $T_1 > T_2$. In general, temperature difference at the interface generates a spin flow from the hotter side to the colder side. When $\Delta T \ll T_1, T_2$, we can expand $L_1/L_2 \approx 1 + (\beta_1 - \beta_2)\varepsilon_q = 1 + \Delta T \frac{\varepsilon_q}{k_B T_1 T_2}$, then $j_d = \mathcal{K}_1 \Delta T$ is proportional to ΔT, and coefficient $\mathcal{K}_1$ is

$$\mathcal{K}_1 = \hbar C \int_{\mathrm{all}} \frac{\varepsilon_q L_2}{k_B T_1 T_2}. \tag{22}$$

To evaluate j_m, we substitute Eq. (9) into Eq. (19) and, noting that $n_1(-\mathbf{q}) = -n_1(\mathbf{q})$, we obtain

$$\begin{aligned} j_m = \alpha_{\mathrm{FI}} \hbar C \int_{\mathrm{all}} \Bigg\{ &\frac{-\tau v_x(\mathbf{q})\varepsilon_q}{k_B T_2^2} L_2 \\ &\times \left[(2n_0 + 1) + \Delta T \frac{\varepsilon_q}{k_B T_1 T_2}(n_0 + 1)\right]\Bigg\}. \end{aligned} \tag{23}$$

For $\Delta T \ll T_1, T_2$, then $L_1/L_2 \approx 1 + \Delta T \frac{\varepsilon_q}{k_B T_1 T_2}$. For the linear response of the spin current to $\Delta T, \alpha_{\mathrm{FI}}$ and α_{NM}, we can drop the last term in the bracket in Eq. (23) that would result in a higher order contribution, proportional to $\Delta T \cdot \alpha_{\mathrm{FI}}$. Note that the integration range includes only $q_x < 0$, thus $-v_x(\mathbf{q}) = -\frac{2J}{\hbar} q_x > 0$, $j_m = \mathcal{K}_2 \alpha_{\mathrm{FI}}$ is proportional to α_{FI}, and coefficient $\mathcal{K}_2$ is

$$\mathcal{K}_2 = \hbar C \int_{\mathrm{all}} \frac{-\tau v_x(\mathbf{q})\varepsilon_q}{k_B T_2^2} L_2(2n_0 + 1), \tag{24}$$

which is positive. When $\alpha_{\mathrm{FI}} > 0$ ($T_L < T_R$), the spin current flows from FI to NM and reverses its direction when $\alpha_{\mathrm{FI}} < 0$. In general, the spin current caused by temperature gradient in FI flows from hotter side to colder side.

In order to compute j_e and because $f_{1,s}$ contains many terms, we decompose j_e into $j_{e,i}$, due to the isotropic part $-\delta\mu_s \frac{\partial f_0(\mathbf{k})}{\partial E}$ of $f_{1,s}$, and $j_{e,a}$, due to the anisotropic part $g_s(\mathbf{k})$ of $f_{1,s}$,

$$\begin{aligned} j_{e,i} = \delta\mu_\uparrow(0) \hbar C \int_{\mathrm{all}} &\beta_1 L_2 \\ &\times \left\{\left(\frac{L_1}{L_2} + 1\right) + \left(\frac{L_1}{L_2} - 1\right)[f_0(\mathbf{k}') - f_0(\mathbf{k}')]\right\} \end{aligned} \tag{25}$$

$$\begin{aligned} j_{e,a} = \hbar C \int_{\mathrm{all}} &\left[a_\uparrow(\mathbf{k})\right](-\beta_1 L_2) \\ &\times \left\{\left(\frac{L_1}{L_2} - 1\right)[1 - f_0(\mathbf{k})] + [1 - 2f_0(\mathbf{k})]\right\} + [a_\downarrow(\mathbf{k}')] \\ &\times (-\beta_1 L_2)\left\{[1 - 2f_0(\mathbf{k}')] - f_0(\mathbf{k}')\left(\frac{L_1}{L_2} - 1\right)\right\}, \end{aligned} \tag{26}$$

where

$$\begin{aligned} a_\uparrow(\mathbf{k}) &= \tau_c v_x(\mathbf{k})\left[\frac{\alpha_{\mathrm{NM}}}{T_1}(E_k - \mu_e) + \frac{\mathrm{d}\mu_e}{\mathrm{d}x} + \frac{\mathrm{d}\delta\mu_\uparrow}{\mathrm{d}x}\right], \\ a_\downarrow(\mathbf{k}') &= \tau_c v_x(\mathbf{k}')\left[\frac{\alpha_{\mathrm{NM}}}{T_1}(E_{k'} - \mu_e) + \frac{\mathrm{d}\mu_e}{\mathrm{d}x} - \frac{\mathrm{d}\delta\mu_\uparrow}{\mathrm{d}x}\right]. \end{aligned} \tag{27}$$

Since $\delta\mu_\uparrow(0)$ is always small, we keeps only linear terms so that all terms with $(\frac{L_1}{L_2} - 1)$ in Eqs. (26), (27) are neglected. Then we have $j_{e,i} \approx \mathcal{K}_3 \delta\mu_\uparrow(0)$ and $j_{e,a} \approx \mathcal{K}_4 \alpha_{\mathrm{NM}} + \mathcal{K}_5 \frac{\mathrm{d}\mu_e}{\mathrm{d}x} +$

$\mathcal{K}_6 \frac{\mathrm{d}\delta\mu_\uparrow}{\mathrm{d}x}$ with coefficients $\mathcal{K}_i$ $(i = 3,4,5,6)$ being

$$\begin{aligned}
\mathcal{K}_3 &= \hbar C \int_{\text{all}} \left(\frac{2L_2}{k_B T_1}\right), \\
\mathcal{K}_4 &= \hbar C \int_{\text{all}} \frac{-\tau_c L_2}{k_B T_1^2}\{v_x(\mathbf{k})(E_k - \mu_e)[1 - 2f_0(\mathbf{k})] \\
&\quad + v_x(\mathbf{k}')(E_{k'} - \mu_e)[1 - 2f_0(\mathbf{k}')]\}, \\
\mathcal{K}_5 &= \hbar C \int_{\text{all}} \frac{-\tau_c L_2}{k_B T_1}\{v_x(\mathbf{k})[1 - 2f_0(\mathbf{k})] \\
&\quad + v_x(\mathbf{k}')[1 - 2f_0(\mathbf{k}')]\}, \\
\mathcal{K}_6 &= \hbar C \int_{\text{all}} \frac{-\tau_c L_2}{k_B T_1}\{v_x(\mathbf{k})[1 - 2f_0(\mathbf{k})] \\
&\quad - v_x(\mathbf{k}')[1 - 2f_0(\mathbf{k}')]\}.
\end{aligned} \tag{28}$$

Note that $\mathcal{K}_4$, $\mathcal{K}_5$, $\mathcal{K}_6$ contain a factor $[1 - 2f_0(\mathbf{k})]$ in the integrals and since only electrons near the Fermi surface participant in scatterings, $[1 - 2f_0(\mathbf{k})]L_2$ is always small. For $\mathcal{K}_5$ and $\mathcal{K}_6$, the factor $(1 - 2f_0) \approx \frac{1}{2}\beta_1(E - \mu_e)$ which change its sign at the Fermi surface, and the contribution from the electrons above and below the Fermi surface almost cancel each other. For $\mathcal{K}_4$, though $(E - \mu_e)(1 - 2f_0) > 0$, but noting that $k_x > 0$ and $k'_x < 0$, the two parts of $\mathcal{K}_4$ have different sign, and their magnitudes are almost the same. According to the previous section, we have $\frac{\mathrm{d}\mu_e}{\mathrm{d}x} = -\frac{\alpha_{NM}}{2T}\frac{(\pi k_B T)^2}{\mu_e}$ and $\frac{\mathrm{d}\delta\mu_\uparrow}{\mathrm{d}x} = \frac{\delta\mu_\uparrow}{l_{sd}}$. The nonequilibrium distribution of electrons would induce a spin current as

$$j_e = j_{e,i} + j_{e,a} = \mathcal{K}'_3\delta\mu_\uparrow(0) + \mathcal{K}'_4\alpha_{NM} \tag{29}$$

where $\mathcal{K}'_3 = \mathcal{K}_3 + \frac{1}{l_{sd}}\mathcal{K}_6$ and $\mathcal{K}'_4 = \mathcal{K}_4 - \frac{T(\pi k_B)^2}{2\mu_e}\mathcal{K}_5$. Numerical results in the next section shows that $\mathcal{K}'_4$ is much smaller than $\mathcal{K}_2$ and almost zero.

C. Spin current injection and spin accumulation at steady state

Substituting results of $j_{\text{FI}\to\text{NM}}$ obtained in the previous subsection and Eq. (14) into Eq. (7), we have

$$\begin{aligned}
&\mathcal{K}_1\ \Delta T + \mathcal{K}_2\alpha_{\text{FI}} + \mathcal{K}'_4\alpha_{\text{NM}} \\
&\quad + \left(\mathcal{K}'_3 + \frac{\hbar}{2e^2}\frac{\sigma}{l_{sd}}\right)\delta\mu_\uparrow(0) = 0,
\end{aligned} \tag{30}$$

and, thus spin accumulation at the FI/NM interface is

$$\begin{aligned}
\delta\mu_\uparrow(0) = &-\frac{2e^2 l_{sd}\mathcal{K}_1}{2e^2 l_{sd}\mathcal{K}'_3 + \hbar\sigma}\Delta T - \frac{2e^2 l_{sd}\mathcal{K}_2}{2e^2 l_{sd}\mathcal{K}'_3 + \hbar\sigma}\alpha_{\text{FI}} \\
&- \frac{2e^2 l_{sd}\mathcal{K}'_4}{2e^2 l_{sd}\mathcal{K}'_3 + \hbar\sigma}\alpha_{\text{NM}}.
\end{aligned} \tag{31}$$

Then the total spin current across the interface is

$$\begin{aligned}
j_{\text{FI}\to\text{NM}} = &\frac{\hbar\sigma\mathcal{K}_1}{\hbar\sigma + 2e^2 l_{sd}\mathcal{K}'_3}\Delta T + \frac{\hbar\sigma\mathcal{K}_2}{\hbar\sigma + 2e^2 l_{sd}\mathcal{K}'_3}\alpha_{\text{FI}} \\
&+ \frac{\hbar\sigma\mathcal{K}'_4}{\hbar\sigma + 2e^2 l_{sd}\mathcal{K}'_3}\alpha_{\text{NM}},
\end{aligned} \tag{32}$$

that flows from the hotter side to the colder side. $\mathcal{K}_1, \mathcal{K}_2, \mathcal{K}'_3, \mathcal{K}'_4$ are functions of T_1 and T_2, which can be determined by Eqs. (22), (24), and (28). T_1 and T_2 are determined by model parameters, as shown in Sec. IV,

$$\begin{aligned}
T_1 &= \frac{T_L(R\kappa_{\text{FI}}\kappa_{\text{NM}} + d_{\text{FI}}\kappa_{\text{NM}}) + T_R d_{\text{NM}}\kappa_{\text{FI}}}{R\kappa_{\text{FI}}\kappa_{\text{NM}} + d_{\text{NM}}\kappa_{\text{FI}} + d_{\text{FI}}\kappa_{\text{NM}}}, \\
T_2 &= \frac{T_L d_{\text{FI}}\kappa_{\text{NM}} + T_R(R\kappa_{\text{FI}}\kappa_{\text{NM}} + d_{\text{NM}}\kappa_{\text{FI}})}{R\kappa_{\text{FI}}\kappa_{\text{NM}} + d_{\text{NM}}\kappa_{\text{FI}} + d_{\text{FI}}\kappa_{\text{NM}}}.
\end{aligned} \tag{33}$$

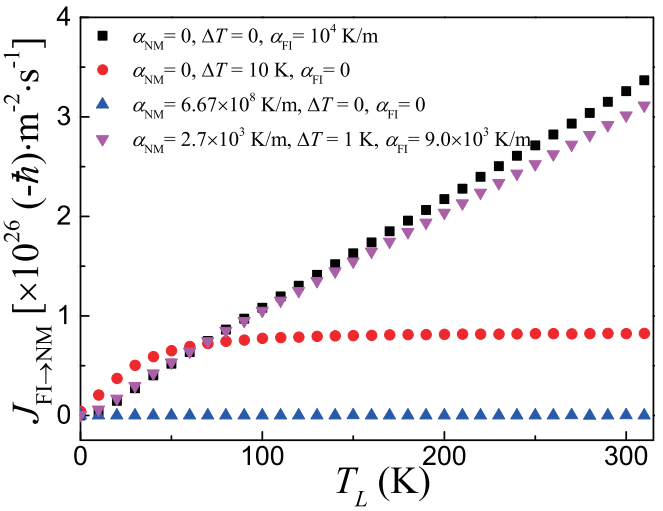

FIG. 2. Spin current $j_{\text{FI}\to\text{NM}}$ as a function of T_L when $T_R = T_L + 10$ K for various sets of α_{NM},α_{FI} and ΔT: $\alpha_{\text{NM}} = 0$,$\alpha_{\text{FI}} = (T_R - T_L)/d_{\text{FI}} = 10^4$ K/m, and $\Delta T = 0$ (black squares); $\alpha_{\text{NM}} = \alpha_{\text{FI}} = 0$, and $\Delta T = 10$ K (red circles); $\alpha_{\text{NM}} = (T_R - T_L)/d_{\text{NM}} = 6.67 \times 10^8$ K/m, $\alpha_{\text{FI}} = 0$, and $\Delta T = 0$ (blue up triangles); $\alpha_{\text{NM}} = 2.7 \times 10^3$ K/m, $\alpha_{\text{FI}} = 9.0 \times 10^3$ K/m, and $\Delta T = 1$ K (magenta down triangles).

V. NUMERICAL RESULTS AND DISCUSSION

To have a better idea about the magnitude of the spin current and spin accumulation generated by a thermal gradient, we numerically compute the total spin current $j_{\text{FI}\to\text{NM}}$ given by Eq. (32) with realistic model parameters of YIG: $S = 23.6, J = 1.9 \times 10^{-40}$ J m^2, $D = 1.8 \times 10^{-24}$ J, $\tau = 10^{-7}$ s [21,33], $b_{\text{FI}} = 1.2$ nm; and Pt: $\sigma = 9.4 \times 10^6$ m^{-1} Ω^{-1}, $l_{sd} = 1.5$ nm, $\mu_0 = 9.74$ eV. $\mathcal{J}_{sd} = 1$ meV, $d_{\text{FI}} = 1$ mm, and $d_{\text{NM}} = 15$ nm [11] are used. The temperature difference between two thermal reservoirs is set to $T_R - T_L = 10$ K. In order to know which thermal source is more effective in spin current generation, we first examine the cases when all 10 K temperature difference is on FI, NM, or at the FI/NM interface. The results are shown in Fig. 2 for $\alpha_{\text{NM}} = 0$, $\alpha_{\text{FI}} = (T_R - T_L)/d_{\text{FI}} = 10^4$ K/m, and $\Delta T = 0$ (black squares); $\alpha_{\text{NM}} = \alpha_{\text{FI}} = 0$, and $\Delta T = T_R - T_L = 10$ K (red circles); $\alpha_{\text{NM}} = (T_R - T_L)/d_{\text{NM}} = 6.67 \times 10^8$ K/m, $\alpha_{\text{FI}} = 0$, and $\Delta T = 0$ (blue up-triangles). Although the thermal gradient in NM ($\alpha_{\text{NM}} = 6.67 \times 10^8$ K/m) is four orders of magnitude larger than that in FI ($\alpha_{\text{FI}} = 10^4$ K/m), the spin current due to α_{NM} (up-triangles) is negligibly smaller than that due to α_{FI} (squares), showing ineffective generation of spin current by the thermal gradient in NM. The magenta down-triangles in Fig. 2 are $j_{\text{FI}\to\text{NM}}$ for $\alpha_{\text{NM}} = 2.7 \times 10^3$ K/m, $\Delta T = 1$ K, and $\alpha_{\text{FI}} = 9.0 \times 10^3$ K/m, corresponding to realistic thermal

conductivities of $\kappa_{\rm FI} = 6.0$ W/(m K) and $\kappa_{\rm NM} = 20$ W/(m K) for YIG and Pt [39], and the interfacial thermal resistance of $R = 1.8 \times 10^{-5}$ K/(W m^{-2}). Interestingly, the spin current generated by a thermal gradient in FI increases almost linearly with the temperature while the spin current under a fixed interfacial temperature difference saturates at a higher enough temperature. We should also notice that spin current generated by a thermal gradient in FI is proportional to the magnon relaxation time, while the spin current under an interfacial temperature difference is not. In reality, when the thermal gradient and the interfacial temperature difference coexist, the proportion of their contributions to the spin current depends on the sample thickness and material parameters.

The experimentally measured ISHE voltage V in open circuit comes from ISHE-induced charge accumulation. According to the above results, when $T_R > T_L$, spins along the $+z$ direction move to the $+x$ direction. Due to the ISHE, a charge current flows along the $+y$ direction (electrons flow to the $-y$ direction), resulting in a charge accumulation in the front/back surfaces (xz planes in Fig. 1) and a higher electric potential in the $+y$ side than that in the $-y$ side as what was observed in experiment [11]. Reversing the direction of either the magnetization of FI or the temperature gradient, the ISHE voltage V changes sign. The effective electric field along the $+y$ direction at the interface can be estimated by [36]

$$\frac{1}{d_{\rm NM}}\int_0^{d_{\rm NM}} j_s(x)\theta_{\rm SH}{\rm d}x = \sigma\mathcal{E}_{\rm avg}, \tag{34}$$

where $\theta_{\rm SH}$ is the spin Hall angle [40] and $V = \mathcal{E}_{\rm avg} w_{\rm NM}$, here $w_{\rm NM}$ is the width of the NM layer. Thus, the voltage is given by

$$|V| = \theta_{\rm SH}\frac{w_{\rm NM}}{d_{\rm NM}}\left|\frac{\delta\mu(0)}{e}\right|. \tag{35}$$

For $w_{\rm NM} = 6$ mm (the same as in the experiment [11]) and for YIG and Pt parameters, the ISHE voltage is estimated to be 60 μV that is larger than the experiment value of 6 μV. The agreement is not too bad since a real system is much more complicated than the ideal model considered here.

In reality, the thermal parameters and relaxation times depend on temperature and the structure of a sample. If these complications can be included, our theory may give a more accurate estimate of the ISHE voltage for a sample. In our analysis, we assume the simplest parabolic energy spectrum and constant relaxation times for magnons and electrons. Though the physics shall not change, the value of all quantities should be sensitive to all these parameters. The interface electron-magnon scattering should be important for other phenomena in FI/NM structures such as spin pumping [2,5–7], transverse SSE [8,9], spin transfer torque on FI [41], and spin Hall magnetoresistance [42]. It may also be relevant to the concept of "spin mixing conductance" [15,20,43].

We investigated the spin transport in a NM/FI system. The spin transport across the interface is via the magnon-electron scattering at the interface, which is modeled by an interfacial s-d coupling between the electrons in NM and magnetic moments in FI. The magnon and electron transports in the bulk are described by Boltzmann equations. Xiao *et al.* [16] used the stochastic LLG equation to model the spin dynamics in FI, and the spin conversion at the interface is modeled by the spin mixing conductance. Adachi *et al.* [19] used a similar s-d model to describe the spin transport across the interface, but only interface temperature difference between the NM and the FI is considered. Zhang *et al.* [21] also used the s-d model and Boltzmann equation to model the interface and bulk transports, but a rough interface is assumed so that the parallel component of momentum is not conserved during the magnon-electron scattering. The anisotropic parts of the magnon and electron distribution functions are also neglected. All these approaches provide meaningful physical pictures for the spin transport in the NM/FI system.

VI. CONCLUSION

It is shown that no spin injection and no spin accumulation are possible at the thermal equilibrium. This conclusion is general and model independent as demanded by the thermodynamical laws. Spin current and spin accumulation can be generated through electron-magnon scatterings by two thermal sources: temperature gradients in FI layers and a temperature difference at NM/FI interface. Both spin current and spin accumulation are sensitive to material properties. The spin accumulation increases and the spin current decreases as the spin diffusion length of NM increases. The spin current arises from imbalance of magnon absorption and emission originated from different magnon and electron temperatures or the deviations of magnons from their equilibrium distributions. Spin current flows from the hotter side to the colder one under a temperature gradient in FI or under an interfacial temperature difference, consistent with existing experiments. In contrast, a temperature gradient in NM cannot efficiently induce a spin current.

ACKNOWLEDGMENTS

This work was supported by National Natural Science Foundation of China (Grant No. 11374249). Hong Kong RGC (Grant No. 163011151 and No. 605413).

APPENDIX: MAGNON TRANSPORT AND ACCUMULATION WITH NONZERO CHEMICAL POTENTIAL

Earlier, we assumed zero magnon chemical potential. In reality, there would be a nonzero magnon chemical potential when the magnon lifetime is finite and much longer than the magnon thermalization time [18,20,33]. Below, we consider two kinds of processes: One is the elastic scatterings which conserves both the magnon number and the magnon energy so that the magnons tend to distribute isotropically. The other is the number-non-conserving scatterings by which the magnons relax to the equilibrium distribution n_0. We show that within this model, there will be a finite magnon accumulation [44,45], and an effective magnon chemical potential can be defined. The value of spin current will change without changing the physics stated in the main text.

For the number conserving processes, the scattering rate is given by the Fermi's golden rule,

$$\Gamma[n] = \sum_{\mathbf{q}'} |W_{\mathbf{q}'\mathbf{q}}|^2 n(\mathbf{r},\mathbf{q}')\delta(\varepsilon_{\mathbf{q}'} - \varepsilon_{\mathbf{q}}) - \sum_{\mathbf{q}'} |W_{\mathbf{q}\mathbf{q}'}|^2 n(\mathbf{r},\mathbf{q})\delta(\varepsilon_{\mathbf{q}} - \varepsilon_{\mathbf{q}'}) \tag{A1}$$

where $n(\mathbf{r},\mathbf{q})$ is the magnon distribution function at position $\mathbf{r}$ and wave vector $\mathbf{q}$, $W_{\mathbf{q}'\mathbf{q}}$ is the matrix element for transition from $\mathbf{q}'$ to $\mathbf{q}$. Γ has to satisfy $\Gamma[n_0] = 0$ so that an equilibrium state is not changed. By substituting n_0 in Eq. (A1), we find $|W_{\mathbf{q}'\mathbf{q}}| = |W_{\mathbf{q}\mathbf{q}'}|$. It is easy to see for any isotropic $n(\mathbf{r},\mathbf{q}) = \bar{n}(\mathbf{r},q)$, the elastic scattering term is 0 ($q = |\mathbf{q}|$ is the magnitude of $\mathbf{q}$). Under a small driving force, we adopt relaxation time approximation [35,44] and the elastic scattering term reads,

$$\Gamma[n] = -\frac{n(\mathbf{r},\mathbf{q}) - \bar{n}(\mathbf{r},q)}{\tau_{\rm el}}, \tag{A2}$$

where $\tau_{\rm el}$ is the elastic scattering time. Because the scattering processes do not change q and the magnon number, we can write

$$\int n(\mathbf{r},\mathbf{q})\mathrm{d}\Omega = \int \bar{n}(\mathbf{r},q)\mathrm{d}\Omega = 4\pi\bar{n}(\mathbf{r},q) \tag{A3}$$

where Ω is the solid angle. The number-non-conserving scattering rate is the same as that in Eq. (8). Thus, the magnon Boltzmann equation is written as

$$\mathbf{v}_{\mathbf{q}} \cdot \nabla n(\mathbf{r},\mathbf{q}) = -\frac{n(\mathbf{r},\mathbf{q}) - \frac{\int n(\mathbf{r},\mathbf{q})\mathrm{d}\Omega}{4\pi}}{\tau_{\rm el}} - \frac{n(\mathbf{r},\mathbf{q}) - n_0}{\tau}. \tag{A4}$$

We can see that when $\tau_{\rm el} \gg \tau$, the first term in the right hand side can be neglected, and Eq. (A4) returns to Eq. (8) in the main text. Here we consider the case $\tau \gg \tau_{\rm el}$, which is true in YIG [20,33,43].

To solve Eq. (A4), we assume the system is infinitely large in y and z directions so that the distribution function only depends on x in real space. We also assume the magnons have a spherical Brillouin zone with the same volume as the cubic one. This assumption is valid because the contribution of high energy magnons is small when the temperature is far from the Curie temperature. The radius of the Brillouin zone q_m satisfies $\frac{4\pi}{3}q_m^3 = (\frac{2\pi}{b_{\rm FI}})^3$. Thus, the system has rotational symmetry around the x direction in $\mathbf{q}$ space. Following Refs. [35,44], within linear response regime, the deviation of distribution function from the equilibrium one can be expanded in Legendre polynomials of $\cos\theta$, where θ is the polar angle between the $\mathbf{q}$ and x axis,

$$n(\mathbf{r},\mathbf{q}) = n(x,q,\cos\theta) = n_0(x,q) + \sum_{n=0}^{\infty} g_n(x,q)P_n(\cos\theta) \tag{A5}$$

where $P_n(\cos\theta)$ is the nth order Legendre polynomial of $\cos\theta$. Substituting the expansion in Eq. (A4), and projecting both sides on $P_m(\cos\theta)$ ($m = 0,1\cdots n$), yields the following equations for each q:

$$\frac{v_q}{3}\frac{\partial g_1}{\partial x} = -\frac{g_0}{\tau}, \tag{A6}$$

$$v_q\left(\frac{\partial n_0}{\partial x} + \frac{\partial g_0}{\partial x} + \frac{2}{5}\frac{\partial g_1}{\partial x}\right) = -\frac{g_1}{\tau'}, \tag{A7}$$

$$\vdots$$

$$v_q\left(\frac{n+1}{2n+3}\frac{\partial g_{n+1}}{\partial x} + \frac{n}{2n-1}\frac{\partial g_{n-1}}{\partial x}\right) = -\frac{g_n}{\tau'}, \tag{A8}$$

where $v_q = \frac{2Jq}{\hbar}$ and $\tau' = (\tau_{\rm el}^{-1} + \tau^{-1})^{-1}$. We first consider the corresponding homogeneous system of (A6)–(A8) ($\frac{\partial n_0}{\partial x} = 0$). The ratio g_{n+1}/g_n is about $\sqrt{\tau'/\tau}$ for $n \geqslant 1$. This can be examined by truncate the series after a finite order and solve all the terms. Since $\tau \gg \tau_{\rm el} > \tau'$, we can ignore g_2 and all higher order terms to obtain

$$g_0(x,q) = \sqrt{\frac{\tau}{3\tau'}}[B_1(q)e^{x/\lambda_q} + B_2(q)e^{-x/\lambda_q}], \tag{A9}$$

$$g_1(x,q) = B_1(q)e^{x/\lambda_q} - B_2(q)e^{-x/\lambda_q}, \tag{A10}$$

where $\lambda_q = v_q\sqrt{\tau\tau'/3}$. The general solution of the nonhomogeneous system (A6)–(A8) is given by the general solution of the homogeneous system plus a particular solution of the nonhomogeneous system,

$$g_0(x,q) = \sqrt{\frac{\tau}{3\tau'}}\left\{\left[B_1(q)e^{\frac{x}{\lambda_q}} + B_2(q)e^{-\frac{x}{\lambda_q}}\right] - \frac{1}{2\lambda_q}\left[e^{\frac{x}{\lambda_q}}\int_0^x F(x',q)e^{-\frac{x'}{\lambda_q}}\mathrm{d}x' + e^{-\frac{x}{\lambda_q}}\int_0^x F(x',q)e^{\frac{x'}{\lambda_q}}\mathrm{d}x'\right]\right\}, \tag{A11}$$

$$g_1(x,q) = B_1(q)e^{\frac{x}{\lambda_q}} - B_2(q)e^{-\frac{x}{\lambda_q}} + \frac{1}{2\lambda_q}\left[e^{\frac{x}{\lambda_q}}\int_0^x F(x',q)e^{-\frac{x'}{\lambda_q}}\mathrm{d}x' - e^{-\frac{x}{\lambda_q}}\int_0^x F(x',q)e^{\frac{x'}{\lambda_q}}\mathrm{d}x'\right]. \tag{A12}$$

where $F(x,q) = \tau' v_q\frac{\partial n_0}{\partial x}$. For each q, the coefficients $B_1(q)$ and $B_2(q)$ are determined by the boundary conditions. At the outer boundary of FI, we assume the magnons are specularly reflected [46],

$$(v_q\cos\theta)n(d_{\rm FI},q,\cos\theta) = (v_q\cos\theta)n(d_{\rm FI},q,-\cos\theta). \tag{A13}$$

At the NM/FI interface, if the magnons are not absorbed or emitted, they are still specularly reflected,

$$\int[(v_q\cos\theta)n(0,q,\cos\theta) - N_{\rm ab}(q,\cos\theta)]d\Omega = \int\left[(v_q\cos\theta)n(0,q,-\cos\theta) - N_{\rm em}(q,\cos\theta)\right]d\Omega. \tag{A14}$$

Here, $N_{\rm ab}(q,\cos\theta)$ and $N_{\rm em}(q,\cos\theta)$ are absorbed and emitted magnon number per unit area for each $\mathbf{q}$,

$$N_{\rm ab}(q,\cos\theta) = C\int f_\uparrow(\mathbf{k})[1-f_\downarrow(\mathbf{k}')]n(\mathbf{q}) \times \delta(E_{\mathbf{k}}+\varepsilon_{\mathbf{q}}-E_{\mathbf{k}'})\delta(\mathbf{k}_\parallel+\mathbf{q}_\parallel-\mathbf{k}'_\parallel)\mathrm{d}\mathbf{k}\mathrm{d}\mathbf{k}', \tag{A15}$$

$$N_{\rm em}(q,\cos\theta) = C\int f_\downarrow(-\mathbf{k}')[1-f_\uparrow(-\mathbf{k})][n(-\mathbf{q})+1] \times \delta(E_{\mathbf{k}}+\varepsilon_{\mathbf{q}}-E_{\mathbf{k}'})\delta(\mathbf{k}_\parallel+\mathbf{q}_\parallel-\mathbf{k}'_\parallel)\mathrm{d}\mathbf{k}\mathrm{d}\mathbf{k}'. \tag{A16}$$

We can numerically solve $B_1(q)$ and $B_2(q)$ for each $q\in[0,q_m]$. The interface spin current is

$$j_{\rm FI\to NM} = \frac{\hbar}{(2\pi)^3}\int_{\cos\theta<0}\int_0^{q_m}[n(0,q,\cos\theta) - n(0,q,-\cos\theta)]q^2\mathrm{d}q\mathrm{d}\Omega. \tag{A17}$$

Figure 3 shows the comparison between the spin currents calculated from the model in the main text and the model in the appendix for $\alpha_{\rm NM}=0,\alpha_{\rm FI}=(T_R-T_L)/d_{\rm FI}=10^4$ K/m, and $\Delta T=0$ and $\alpha_{\rm NM}=\alpha_{\rm FI}=0$, and $\Delta T=10$ K. We take $\tau_{\rm el}=10^{-8}$ s and all other parameters are the same as those in the main text. Under the temperature difference, the results here are slightly larger than the results in the main text. Under the temperature gradient, at low temperature (<40 K), the results here are closed to the results in the main text; however, when the temperature is higher, the results here are much lower than the results in the main text.

The magnon accumulation [44] can be calculated by

$$\delta N(x) = N(x) - N_0(x) = \frac{1}{(2\pi)^3}\int g_0(x,q)\mathrm{d}^3\mathbf{q}. \tag{A18}$$

We can also define an effective magnon chemical potential μ_m via

$$\delta N(x) = \frac{1}{(2\pi)^3}\int\left[\frac{1}{e^{\beta(\varepsilon_q-\mu_m(x))}-1}-\frac{1}{e^{\beta\varepsilon_q}-1}\right]\mathrm{d}^3\mathbf{q}. \tag{A19}$$

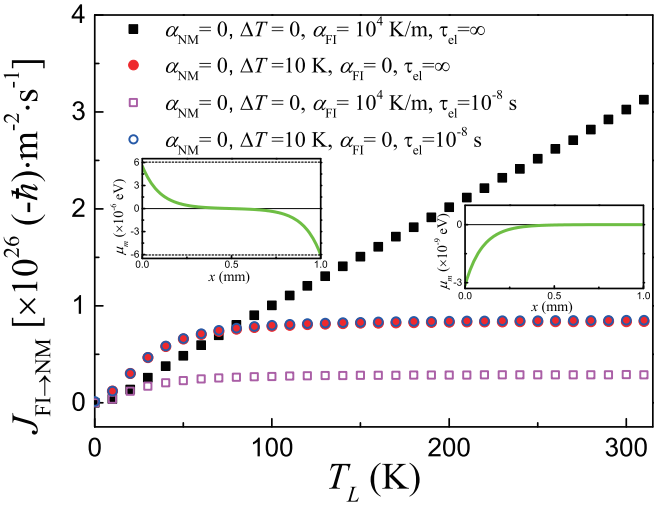

FIG. 3. Comparison of spin current $j_{\rm FI\to NM}$ as a function of T_L when $T_R=T_L+10$ K for $\alpha_{\rm NM}=0,\alpha_{\rm FI}=10^4$ K/m, and $\Delta T=0$ (black solid squares and blue hollow squares); $\alpha_{\rm NM}=\alpha_{\rm FI}=0$, and $\Delta T=10$ K (red solid circles and magenta hollow circles). The solid symbols are the results in the main text. The hollow symbols are the results with $\tau_{\rm el}=10^{-8}$ s. Left inset: Spatial profile of μ_m for $\alpha_{\rm NM}=0$, $\alpha_{\rm FI}=10^4$ K/m, and $\Delta T=0$ at $T_L=300$ K. The dashed lines denote the value of $\pm\mu_m(d_{\rm FI})$. Right inset: Spatial profile of μ_m for $\alpha_{\rm NM}=\alpha_{\rm FI}=0$, and $\Delta T=10$ K at $T_L=300$ K.

The spatial profiles of μ_m are plotted in the insets of Fig. 3 for $T_L=300$ K. The left inset is for $\Delta T=0$ and $\alpha_{\rm FI}=10^4$ K/m. The magnons accumulate at the NM/FI interface with a positive μ_m. At the outer boundary of FI, μ_m is negative and the diffusion current completely cancels the thermal-gradient driven current. $\mu_m(0)<-\mu_m(d_{\rm FI})$ because some of the magnons are absorbed by the NM through the interface. If the temperature gradient reverses the direction, magnons will deplete at the NM/FI interface with a negative μ_m. When we consider longer magnon lifetime τ than the number-conserving scattering time $\tau_{\rm el}$, there are two effects: A nonzero effective chemical potential increases magnon absorption by electrons so that the interface spin current becomes bigger. On the other hand, the diffusion current due to the nonzero chemical potential is always opposite to the thermal-driven current, resulting in more magnon emissions so that the interface spin current is reduced. The numerical results show that the second effect is more important. The right inset is for $\Delta T=10$ K and $\alpha_{\rm FI}=10^4$ K/m. The magnons deplete at the NM/FI interface with a tiny negative μ_m. This depletion induces a diffusion current in the bulk.

[1] I. Žutić, J. Fabian, and S. Das Sarma, Rev. Mod. Phys. **76**, 323 (2004).

[2] Y. Kajiwara, K. Harii, S. Takahashi, J. Ohe, K. Uchida, M. Mizuguchi, H. Umezawa, H. Kawai, K. Ando, K. Takanashi, S. Maekawa, and E. Saitoh, Nature (London) **464**, 262 (2010).

[3] P. Yan, X. S. Wang, and X. R. Wang, Phys. Rev. Lett. **107**, 177207 (2011); D. Hinzke and U. Nowak, *ibid.* **107**, 027205 (2011); A. A. Kovalev and Y. Tserkovnyak, Europhys. Lett. **97**, 67002 (2012).

[4] X. S. Wang, P. Yan, Y. H. Shen, G. E. W. Bauer, and X. R. Wang, Phys. Rev. Lett. **109**, 167209 (2012); B. Hu and X. R. Wang, *ibid.* **111**, 027205 (2013).

[5] C. W. Sandweg, Y. Kajiwara, K. Ando, E. Saitoh, and B. Hillebrands, Appl. Phys. Lett **97**, 252504 (2010).

[6] B. Heinrich, C. Burrowes, E. Montoya, B. Kardasz, E. Girt, Y.-Y. Song, Y. Sun, and M. Wu, Phys. Rev. Lett. **107**, 066604 (2011).
[7] M. Weiler, M. Althammer, M. Schreier, J. Lotze, M. Pernpeintner, S. Meyer, H. Huebl, R. Gross, A. Kamra, J. Xiao, Y. T. Chen, H. J. Jiao, G. E. W. Bauer, and S. T. B. Goennenwein, Phys. Rev. Lett. **111**, 176601 (2013).
[8] K. Uchida, S. Takahashi, K. Harii, J. Ieda, W. Koshibae, K. Ando, S. Maekawa, and E. Saitoh, Nature (London) **455**, 778 (2008).
[9] K. Uchida, J. Xiao, H. Adachi, J. Ohe, S. Takahashi, J. Ieda, T. Ota, Y. Kajiwara, H. Umezawa, H. Kawai, G. E. W. Bauer, S. Maekawa, and E. Saitoh, Nat. Mater. **9**, 894 (2010).
[10] C. M. Jaworski, J. Yang, S. Mack, D. D. Awschalom, R. C. Myers, and J. P. Heremans, Phys. Rev. Lett. **106**, 186601 (2011).
[11] K. Uchida, M. Ishida, T. Kikkawa, A. Kirihara, T. Murakami, and E. Saitoh, J. Phys. Condens. Matter **26**, 343202 (2014).
[12] D. Qu, S. Y. Huang, J. Hu, R. Wu, and C. L. Chien, Phys. Rev. Lett. **110**, 067206 (2013).
[13] E. Saitoh, M. Ueda, H. Miyajima, and G. Tatara, Appl. Phys. Lett. **88**, 182509 (2006).
[14] G. E. W. Bauer, E. Saitoh, and B. J. van Wees, Nat. Mater. **11**, 391-399 (2012).
[15] Y. Tserkovnyak, A. Brataas, and G. E. W. Bauer, Phys. Rev. Lett. **88**, 117601 (2002).
[16] J. Xiao, G. E. W. Bauer, K.-c. Uchida, E. Saitoh, and S. Maekawa, Phys. Rev. B **81**, 214418 (2010).
[17] S. Hoffman, K. Sato, and Y. Tserkovnyak, Phys. Rev. B **88**, 064408 (2013).
[18] S. A. Bender and Y. Tserkovnyak, Phys. Rev. B **91**, 140402(R) (2015).
[19] H. Adachi, J.-i. Ohe, S. Takahashi, and S. Maekawa, Phys. Rev. B **83**, 094410 (2011); H. Adachi and S. Maekawa, J. Korean Phys. Soc. **62**, 1753 (2013).
[20] S. A. Bender, R. A. Duine, and Y. Tserkovnyak, Phys. Rev. Lett. **108**, 246601 (2012).
[21] S. S.-L. Zhang and S. Zhang, Phys. Rev. B **86**, 214424 (2012).
[22] J. Ren, Phys. Rev. B **88**, 220406(R) (2013).
[23] S. Y. Huang, W. G. Wang, S. F. Lee, J. Kwo, and C. L. Chien, Phys. Rev. Lett. **107**, 216604 (2011); S. Y. Huang, X. Fan, D. Qu, Y. P. Chen, W. G. Wang, J. Wu, T. Y. Chen, J. Q. Xiao, and C. L. Chien, *ibid.* **109**, 107204 (2012).
[24] T. A. Kaplan, Phys. Rev. **109**, 782 (1958).
[25] G. Grosso and G. P. Parravicini, *Solid State Physics* (Elsevier, Waltham, 2014).
[26] D. A. Goodings, Phys. Rev. **132**, 542 (1963).
[27] T. Holstein and H. Primakoff, Phys. Rev. **58**, 1098 (1940).
[28] A. Miller and E. Abrahams, Phys. Rev. **120**, 745 (1960).
[29] A. Vedyayev, N. Ryzhanova, N. Strelkov, and B. Dieny, Phys. Rev. Lett. **110**, 247204 (2013).
[30] J. Lu, S. Yin, L. M. Peng, Z. Z. Sun, and X. R. Wang, Appl. Phys. Lett. **90**, 052109 (2007).
[31] E. T. Swartz and R. Q. Pohl, Rev. Mod. Phys. **61**, 605 (1989).
[32] M. Schreier, A. Kamra, M. Weiler, J. Xiao, G. E. W. Bauer, R. Gross, and S. T. B. Goennenwein, Phys. Rev. B **88**, 094410 (2013).
[33] S. O. Demokritov, V. E. Demidov, O. Dzyapko, G. A. Melkov, A. A. Serga, B. Hillebrands, and A. N. Slavin, Nature (London) **443**, 430 (2006); O. Dzyapko, V. E. Demidov, S. O. Demokritov, G. A. Melkov, and A. N. Slavin, New J. Phys. **9**, 64 (2007).
[34] S. Zhang, Phys. Rev. Lett. **85**, 393 (2000).
[35] T. Valet and A. Fert, Phys. Rev. B **48**, 7099 (1993).
[36] O. Mosendz, V. Vlaminck, J. E. Pearson, F. Y. Fradin, G. E. W. Bauer, S. D. Bader, and A. Hoffmann, Phys. Rev. B **82**, 214403 (2010).
[37] M. R. Sears and W. M. Saslow, Phys. Rev. B **85**, 014404 (2012).
[38] D. K. C. MacDonald, *Thermoelectricity: an Introduction to the Principles* (Dover Publications, New York, 2006).
[39] Q. G. Zhang, B. Y. Cao, X. Zhang, M. Fujii, and K. Takahashi, J. Phys. Condens. Matter **18**, 7937 (2006); A. M. Hofmeister, Phys. Chem. Miner. **33**, 45 (2006).
[40] L. Q. Liu, T. Moriyama, D. C. Ralph, and R. A. Buhrman, Phys. Rev. Lett. **106**, 036601 (2011).
[41] X. Jia, K. Liu, K. Xia, and G. E. W. Bauer, Europhys. Lett. **96**, 17005 (2011).
[42] H. Nakayama, M. Althammer, Y. T. Chen, K. Uchida, Y. Kajiwara, D. Kikuchi, T. Ohtani, S. Geprags, M. Opel, S. Takahashi, R. Gross, G. E. W. Bauer, S. T. B. Goennenwein, and E. Saitoh, Phys. Rev. Lett. **110**, 206601 (2013).
[43] B. Flebus, S. A. Bender, Y. Tserkovnyak, and R. A. Duine, Phys. Rev. Lett. **116**, 117201 (2016).
[44] S. S.-L. Zhang and S. Zhang, Phys. Rev. Lett. **109**, 096603 (2012).
[45] L. J. Cornelissen, K. J. H. Peters, R. A. Duine, G. E. W. Bauer, and B. J. van Wees, arXiv:1604.03706.
[46] C. Cercignani, *The Boltzmann Equation and its Applications* (Springer-Verlag, New York, 1988).